Available online at www.sciencedirect.com

ScienceDirect

Journal of Energy Chemistry 23(2014)633–638

www.elsevier.com/journals/
journal-of-energy-chemistry/2095-4956
www.elsevier.com/locate/jngc

Effect of Ni loadings on the activity and coke formation of MgO-modified Ni/Al_2O_3 nanocatalyst in dry reforming of methane

Zahra Alipour[a], Mehran Rezaei[a,b*], Fereshteh Meshkani[a]

a. Catalyst and Advanced Materials Research Laboratory, Chemical Engineering Department, Faculty of Engineering, University of Kashan, Kashan 87317-51167, Iran; b. Institute of Nanoscience and Nanotechnology, University of Kashan, Kashan 87317-51167, Iran

[Manuscript received February 14, 2014; revised April 9, 2014]

Abstract

MgO-modified Ni/Al_2O_3 catalysts with different Ni loadings were prepared and employed in dry reforming of methane (DRM). The effect of Ni loadings on the activity and coke formation of Ni/MgO-Al_2O_3 catalysts were investigated. The synthesized catalysts were characterized by XRD, N_2 adsorption-desorption, SEM, TPO and TPR techniques. The obtained results showed that increasing nickel loading decreased the BET surface area and increased the catalytic activity and amount of deposited carbon. In addition, the effect of gas hourly space velocity (GHSV) and feed ratio were studied.

Key words

nickel catalyst; MgO modifier; syngas; dry reforming; coke formation

1. Introduction

Concerns about the depletion of petroleum reserves and consideration on the chemical recycling of CO_2 to fuels/chemicals warrant increasing attention for the catalytic process of CO_2 reforming of CH_4 (also known as dry reforming of methane, DRM, Equation (1)), which can convert two undesirable greenhouse gases into synthesis gas [1,2].

$$CH_4 + CO_2 \rightarrow 2H_2 + 2CO \quad \triangle H_{298} = 247 \text{kJ} \cdot \text{mol}^{-1} \tag{1}$$

This process offers certain advantages, such as a lower H_2/CO ratio, and seems to be more suitable for the Oxo and Fischer-Tropsch processes. The major drawback of this reaction, however, is the rapid deactivation of nickel catalysts as a result of carbon deposition via the Boudouard reaction ($2CO \leftrightarrow C+CO_2$) and/or CH_4 decomposition [3−5]. Therefore, activity and selectivity to syngas, H_2/CO molar ratio, carbon deposit and also specific surface area, dispersion stability and morphological characteristics of the catalysts have been identified as the important parameters that influence the high-performance for synthesis gas. Numerous materials like Ni, Co, Fe and noble metals (Pt, Rh, Pd, Ir) have been reported to be active for CH_4 reforming [6−8]. Although the noble metal-based catalysts are generally reported more active to reactant conversion and less sensitive to carbon deposition, their application is confined by high cost and limited availability. From the commercial viewpoint, industrial practice relies on Ni-based catalysts. However, the major challenge of using Ni-based catalysts is the high thermodynamic potential to carbon deposition, which will not only induce the deactivation of catalysts, but also crush the catalysts pellets, increase the pressure drop, and even block the reactor. Thus, carbon deposition has been the primary hindrance on the way to industrialization of DRM process [1,9−11].

Increasing the concentration of Lewis basicity of the support enhances the chemisorption of CO_2 in CRM reaction. Hence, the alkali metal oxides (such as K_2O, etc.) and alkaline earth metal oxides (such as MgO, CaO and BaO) are commonly chosen as basic supports or modifiers. On one hand, the presence of the basic modifiers promotes the process of eliminating the coke through the course that CO_2 reacts with the C to form CO, improving the stability of the catalyst. On the other hand, the chemisorption of CO_2 activates CO_2 molecule and augments the concentration of CO_2 on the surface of the catalyst, which is beneficial to boost the catalytic activity of the catalyst [12−16].

Considering the above research results, in this work, the effect of Ni loadings on the catalytic activity and coke formation of Ni/MgO-Al_2O_3 catalysts were discussed.

---

[*] Corresponding author. Tel: +98-361-5912469; Fax: +98-361-5559930; E-mail: rezaei@kashanu.ac.ir

This work was supported by the University of Kashan (Grant No. 158426/16).

doi: 10.1016/S2095-4956(14)60194-7

2. Experimental

2.1. Catalyst preparation

γ-Al_2O_3 as catalyst support was prepared according to the method described in our previous work [2]. In summary, aluminum tri isopropylate (98% purity, Merck) was firstly hydrolyzed in distilled water by stirring for 1 h at 80−85 °C. Subsequently, HNO_3 was added dropwise with HNO_3 to Al molar ratio of 1 : 1 and refluxed for 12 h at 98 °C. After that the sol was kept at 98 °C for 2 h in air. After this step the sol was became so viscous. The formed gel was dried overnight at 80 °C and calcined at 600 °C for 4 h. After that, the prepared γ-Al_2O_3 was first impregnated with an aqueous solution of MgO precursor ($Mg(NO_3)_2 \cdot 6H_2O$) with appropriate concentration to obtain 3 wt% of promoter. After impregnation, the promoted support was dried at 80 °C overnight and calcined at 700 °C for 4 h. Then the promoted γ-$Al_2O_3$was impregnated with nickel nitrate with appropriate concentration to obtain different loadings of nickel (5 wt%, 10 wt%, 15 wt% and 20 wt%). Finally, the catalysts were dried at 80 °C overnight and calcined at 500 °C for 4 h.

2.2. Characterization

X-ray diffraction (XRD) analysis was performed using an X-ray diffractometer (PANalyticalX'Pert-Pro) with a Cu-K_α monochromatized radiation source and a Ni filter in the range of $2\theta = 10^o$–70^o to examine the crystallinity of the prepared samples. N_2 adsorption/desorption analysis was carried out at boiling temperature of nitrogen (−196 °C) using an automated gas adsorption analyzer (Tristar 3020, Micromeritics). The samples were purged with nitrogen gas for 2 h at 200 °C using VacPrep 061 degas system (Micromeritics). Temperature-programmed reduction (TPR) analysis was used for evaluating the reduction properties of the prepared catalysts with Micromeritics chemisorb 2750 gas-adsorption equipment. In TPR measurement, 100 mg catalyst was subjected to a heat treatment (10 °C/min) in a gas flow (30 mL/min) containing a mixture of H_2 : Ar (10 : 90). Prior to TPR experiment, the samples were heat treated under an inert atmosphere (Ar) at 200 °C for 1 h. H_2 uptake amount during the reduction was measured using a thermal conductivity detector (TCD). Temperature-programmed oxidation (TPO) of the spent catalysts was carried out using a similar apparatus by introducing a gas flow (30 mL/min) containing a mixture of O_2 and He (5 : 95) and the temperature was increased up to 800 °C at a heating rate of 10 °C/min. Scanning electron microscopy (SEM) analysis was performed with VEGA TESCAN operated at 30 kV.

2.3. Catalysts evaluation

The catalytic reaction was carried out in a tubular fixed bed flow reactor made of quartz under atmospheric pressure. The thermocouple was inserted in the bottom of the catalyst bed to monitor the temperature. The reactor was charged with 200 mg of the prepared catalyst. Prior to reaction, the catalysts were reduced with the flow of pure H_2 gas (GHSV = 6000 mL/($g_{cat} \cdot$h)) at a heating rate of 10 °C/min from room temperature to 600 °C and then maintained at 600 °C for 2 h. The reactant gas stream consisting of CH_4 and CO_2 with constant molar ratios, was controlled by mass flow controller and the activity tests were carried out at different temperatures ranging from 550 to 700 °C in steps of 50 °C. The reaction effluents were analyzed using a gas chromatograph (Varian 3400) equipped with a TCD and a carboxen 1000 column.

3. Results and discussion

3.1. Structural properties of the catalysts

Figure 1 shows the XRD patterns of NiO/MgO-Al_2O_3 catalysts with different Ni loadings. It can be seen that by increasing Ni loading, two peaks were detected at $2\theta = 43.5^o$ and 75.6^o, which are ascribed to NiO phase. These extra peaks were not observed when Ni loadings were 5 wt% and 10 wt%, due to low percentage of Ni in these two catalysts. Also increasing nickel loading decreased the fraction of $NiAl_2O_4$ at $2\theta = 67^o$ that overlapped with Al_2O_3 phase. Increasing Ni contents causes an increase in Ni crystallite size and consequently a decrease in Ni dispersion. Therefore, peaks appear intensely for high nickel loadings.

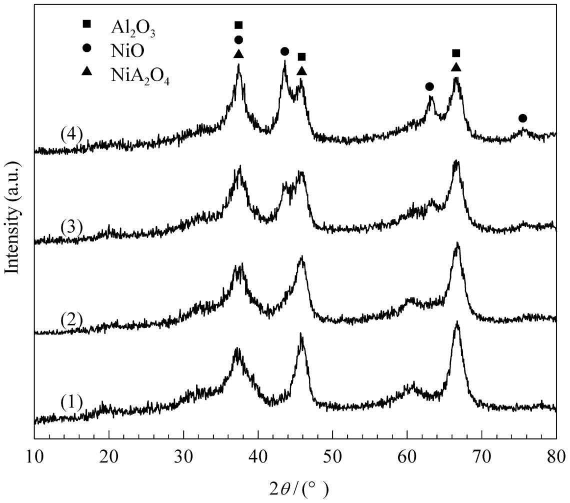

Figure 1. XRD patterns of NiO/3 wt% MgO-Al_2O_3 catalysts with various Ni loadings. (1) 5 wt%, (2) 10 wt%, (3) 15 wt%, (4) 20 wt%

The structural properties of NiO/MgO-Al_2O_3 catalysts with different Ni contents are summarized in Table 1. It is seen that, increasing Ni loading decreased S_{BET} and pore volume. The decrease in BET surface area and pore volume is due to the blocking of catalyst pores with loaded nickel. Figure 2(a) displays the nitrogen adsorption/desorption isotherms of these catalysts. All the samples showed IV type isotherm with H2 shaped hysteresis loop, indicating the mesoporous features. The H2 shaped hysteresis loops generally illuminated that all the mesopores were cylindrical-shaped channels with non-uniform pores [8]. Furthermore, the pore size distributions of these samples are presented in Figure 2(b). It is seen that all the samples showed a mesoporous structure with a pore size located in the range of 5−16 nm. As seen, increasing nickel loading shifted the pore size distribution to smaller size.

Table 1. Structural properties of NiO/3 wt% MgO-Al_2O_3 catalysts with different Ni loadings

Ni loadings	S^{a}_{BET} (m^2/g)	Pore volume^{b} (cm^3/g)	Pore width^{c} (nm)
5 wt%	153	0.44	8.6
10 wt%	140	0.39	8.6
15 wt%	133	0.35	8.4
20 wt%	121	0.32	8.0

[a] Calculated by BET equation; [b] BJH desorption pore volume; [c] BJH desorption average pore diameter

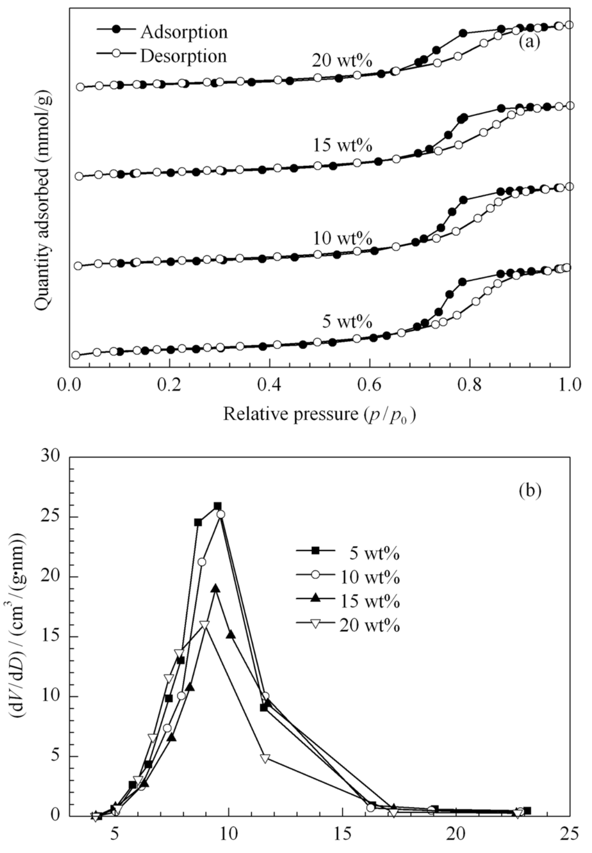

Figure 2. N_2 adsorption/desorption isotherms (a) and pore size distributions (b) of calcined NiO/3 wt%MgO-Al_2O_3 catalysts with different Ni loadings

3.2. TPR analysis

TPR profiles of NiO/MgO-Al_2O_3 catalysts with various Ni contents are shown in Figure 3. All the samples showed only one remarkable reduction peak in the region of 600 °C to 770 °C regardless of Ni content. The reduction peak for dissociated NiO also did not appear in the low temperature region (300−400 °C) either, suggesting that the intense interaction between Ni species and the support had also been established [12]. In addition, as the Ni loading decreased from 20 wt% to 5 wt%, the hydrogen uptake peaks decreased because of the decrease of Ni content. Moreover, the reduction peak gradually migrated towards lower temperature as the Ni loading increased, which might be related to the lower interaction between nickel and catalyst support due to the increasing Ni particle size.

The second peak observed at about 900 °C, can be attributed to $NiAl_2O_4$ species. As seen, with the increase of Ni loading, the peak intensity was reduced and shifted to lower temperatures. It can be concluded that by increasing Ni content, NiO phase appeared more than $NiAl_2O_4$ phase and the catalyst reducibility was improved.

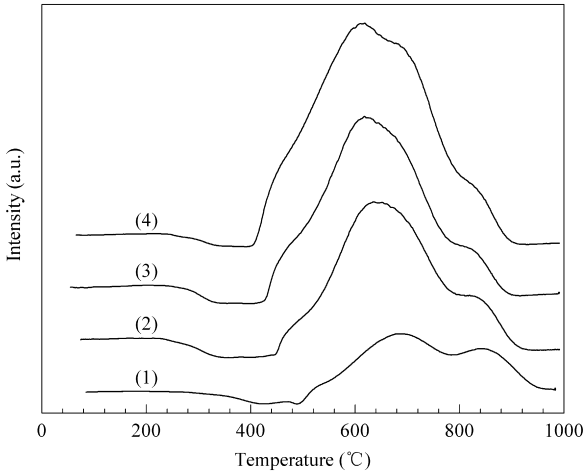

Figure 3. TPR profiles of NiO/3 wt%MgO-Al_2O_3 catalysts with different Ni loadings. (1) 5 wt%, (2) 10 wt%, (3) 15 wt%, (4) 20 wt%

3.3. Catalytic performance

The effect of Ni content on the catalytic activity of NiO/3 wt%MgO-Al_2O_3 catalyst was studied. CH_4 and CO_2 conversions of the prepared catalysts are shown in Figure 4(a) and 4(b), respectively. As seen, both CH_4 and CO_2 conversions increased in the temperature range of 550−700 °C due to the endothermic nature of CRM reaction. It was found that the conversion of CH_4 increased with the increase of Ni loading from 5 wt% to 20 wt%, suggesting that more active sites were provided as Ni loading increased. H_2/CO molar ratios of the catalysts are shown in Figure 4(c). It is clear that H_2/CO ratio was less than one for all the samples due to the presence of reverse water gas shift reaction ($CO_2+H_2 \leftrightarrow CO+H_2O$).

Short time stability test was carried out on NiO/3 wt%MgO-Al_2O_3 catalysts at 700 °C. As it is demonstrated in Figure 5(a), all these catalysts displayed a very high stability without any decrease in CH_4 conversion over the test period of 300 min. Long term stability was performed over

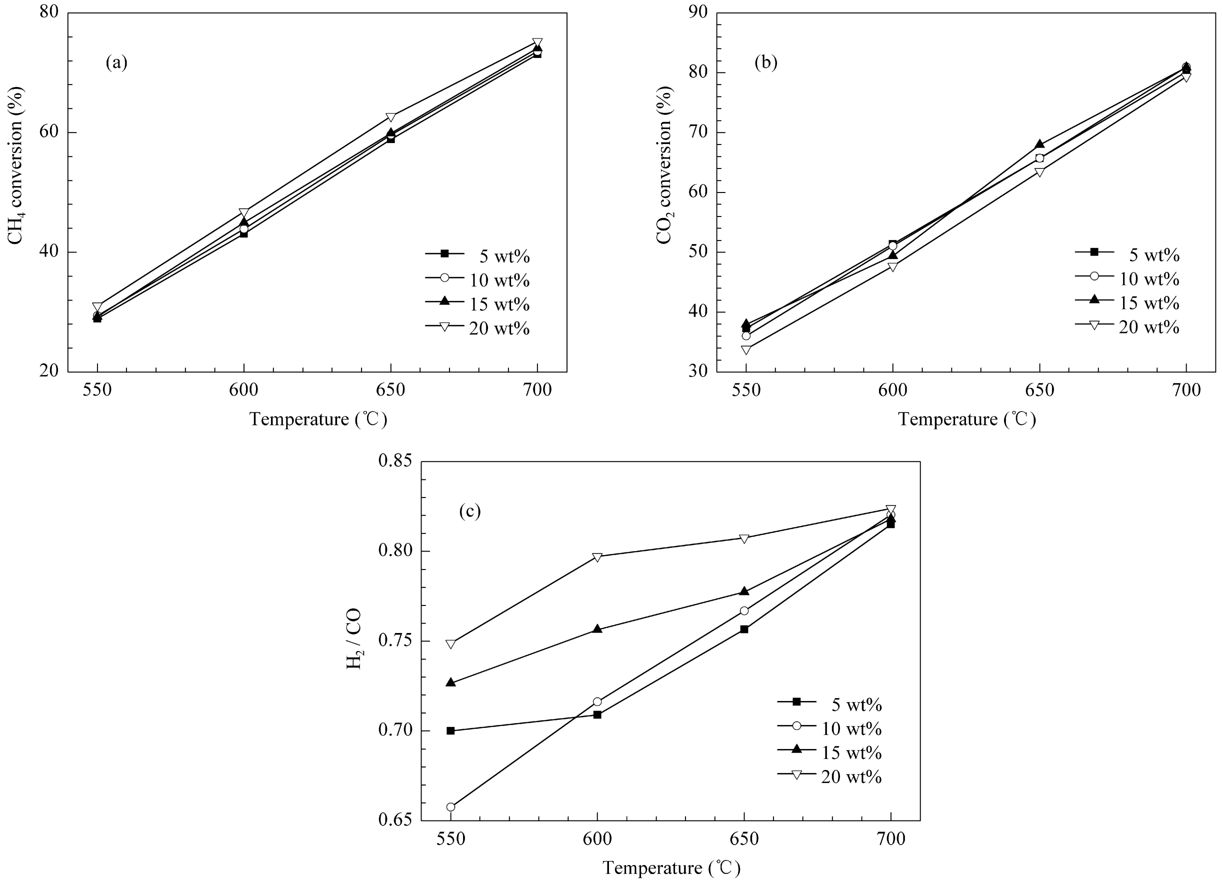

Figure 4. CH_4 conversion (a), CO_2 conversion (b) and H_2/CO ratio (c) on NiO/3 wt%MgO-Al_2O_3 catalysts with different Ni loadings in dry reforming of methan. Reaction conditions: $CH_4/CO_2 = 1/1$, GHSV = 12000 mL/(g_{cat}·h)

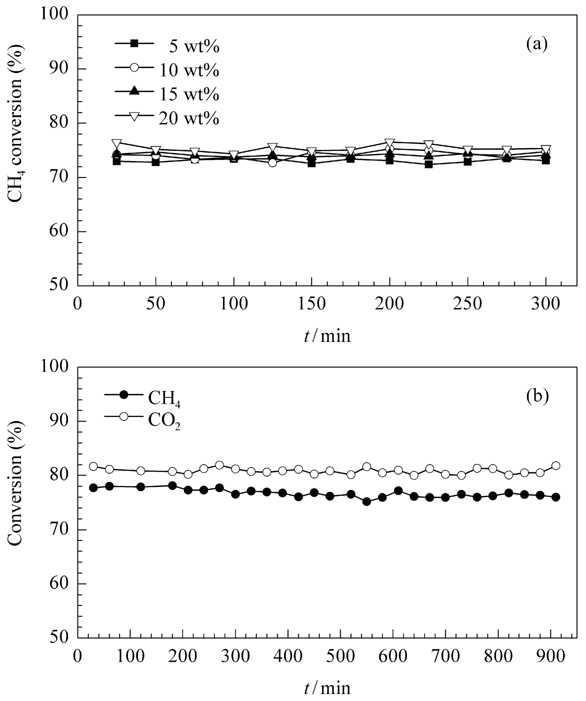

Figure 5. Short time stability of Ni/3 wt%MgO-Al_2O_3 catalysts with various Ni loadings (a) and long term stability of Ni/3 wt%Mg-Al_2O_3 catalyst with 20 wt% Ni loading (b). Reaction conditions: $CH_4 : CO_2 = 1 : 1$, $T = 700$ °C and GHSV = 12000 mL/(g_{cat}·h)

the catalyst with 20 wt% Ni loading (Figure 5b). The result showed that this catalyst has a high stability during 15 h time on-stream under the reaction conditions.

The effect of gas hour space velocity (GHSV) on the catalytic performance of 20 wt%Ni/3 wt%MgO-Al_2O_3 catalyst was studied by maintaining the reaction temperature and feed ratio in the system constant ($T = 650$ °C, $CH_4 : CO_2 = 1 : 1$). Figure 6 demonstrates that with the increase of GHSV from 6000 to 18000 mL/(g_{cat}·h), the conversions of CH_4 and CO_2

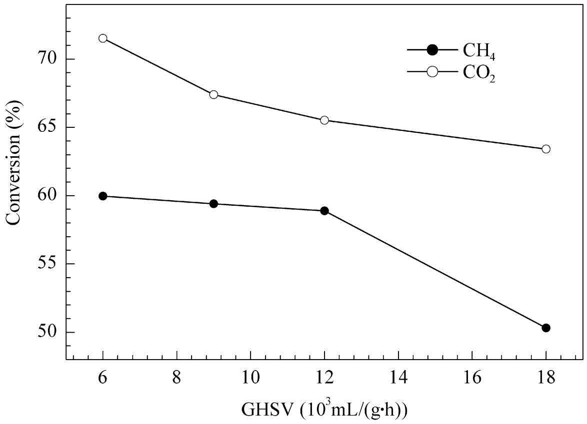

Figure 6. Effect of GHSV on the catalytic activity of 20 wt%Ni/3 wt%MgO-Al_2O_3 catalyst. Reaction conditions: $CH_4/CO_2 = 1 : 1$, $T = 650$ °C

decreased. The reason for this might derive from the reduction in the residence time of the reactants on the surface of the catalysts. As a result, the thermodynamic equilibrium could not be achieved due to the insufficient contact time, leading to the decrease of the catalytic activity [12].

Figure 7 presents the effect of feed ratio on the catalytic activity of 20 wt%Ni/3 wt%MgO-Al_2O_3 catalyst at 650 °C. The results showed that with an increase in CH_4 to CO_2 ratio from 1 : 4 to 4 : 1, CH_4 conversion decreased whereas CO_2 conversion increased (Figure 7a). The ratio of H_2/CO also increased with the increase of CH_4/CO_2 ratio, since the water gas shift reaction took place seriously at a lower ratio of CH_4/CO_2 (Figure 7b).

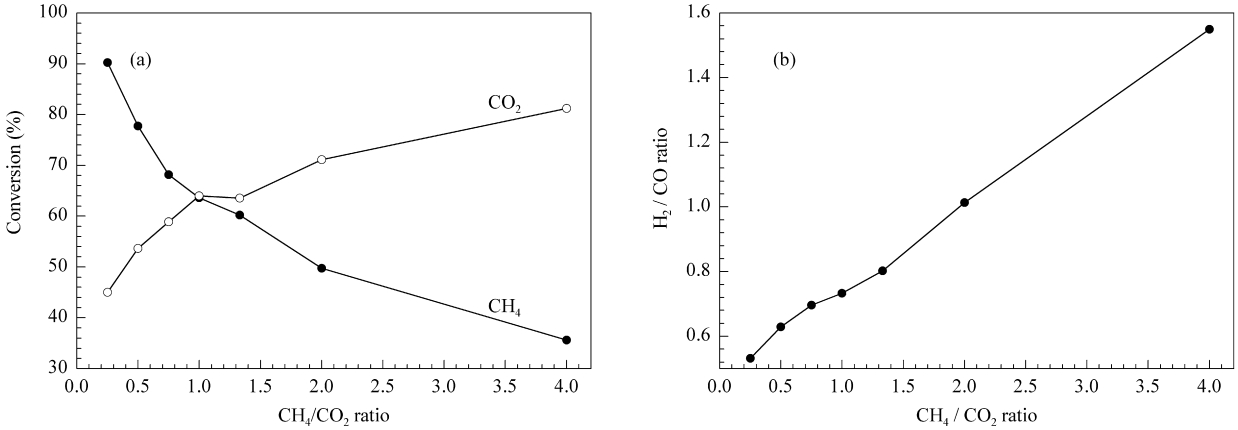

Figure 7. Effect of feed ratio on the catalytic performance of 20 wt%Ni/3 wt%MgO-Al_2O_3 at 650 °C and GHSV = 12000 mL/(g_{cat}·h). (a) CH_4 and CO_2 conversion, (b) H_2/CO ratio

3.4. TPO analysis

TPO profiles of the spent Ni/MgO-Al_2O_3catalysts with different nickel loadings are shown in Figure 8. It is seen that two oxidation peaks were detected for all the catalysts, indicative of two kinds of carbonaceous species formed on the catalysts. The first small peak at very low temperature could be related to the extremely reactive carbonaceous species [12]. The high temperature peak around 700 °C could be ascribed to filamentous carbon [17]. The obtained results showed that with an increase of Ni loading the intensity of peak in these profiles increased because of an increase in the amount of deposited carbon. The highest amount of deposited carbon was observed over the 20 wt%Ni/3 wt%MgO-Al_2O_3 catalyst, which may be related to the fact that this catalyst had the largest particle size and the lowest Ni dispersion.

Increase in the coke deposition over the catalysts with higher nickel loadings could be related to the lower dispersion of nickel on the catalysts with higher nickel loadings [10].

TPO profile of 20%Ni/3%MgO-Al_2O_3 spent catalyst after 15 h reaction is shown in Figure 8(b). As seen, one kind of carbon specie deposited on the catalyst surface during CRM reaction, which is corresponding to the whisker carbon.

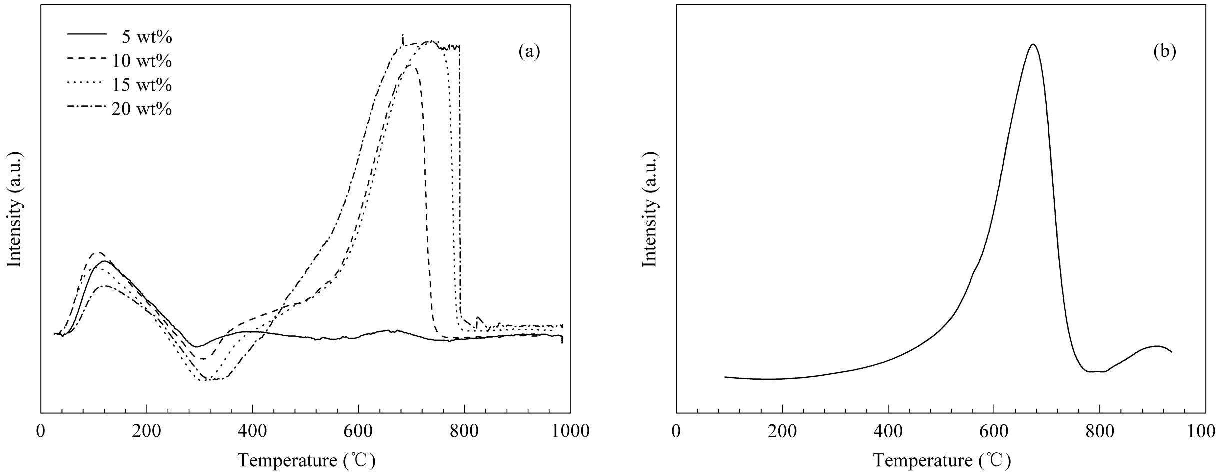

Figure 8. TPO profiles of Ni/3 wt%MgO-Al_2O_3 with different Ni loadings (a) and 20 wt%Ni/3%MgO-Al_2O_3 spent catalyst after 15 h reaction (b). Reaction conditions: $CH_4 : CO_2 = 1 : 1$, T = 700 °C, GHSV = 12000 mL/(g_{cat}·h) and time on stream = 15 h

3.5. SEM analysis

SEM results of Ni/MgO-Al_2O_3 catalysts with 5 wt% and 20 wt% Ni loading are presented in Figure 9. It is obvious that the amount of filamentous carbon formed over the catalyst with 20 wt% nickel was higher compared to that with 5 wt% nickel, due to lower dispersion of nickel over the catalyst with higher nickel loading. This is in agreement with TPO results, which showed higher amount of deposited carbon over the catalysts with higher nickel loadings.

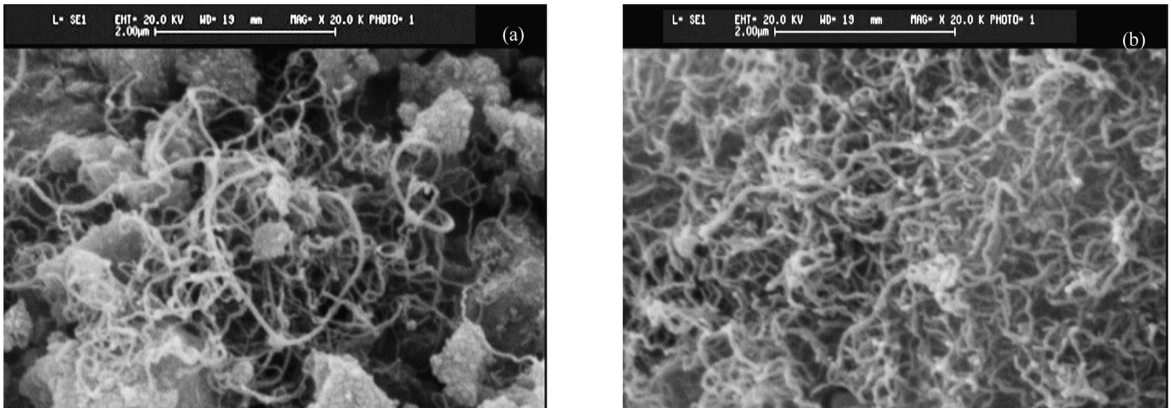

Figure 9. SEM images of (a) 5 wt%Ni/3 wt%MgO-Al_2O_3 and (b) 20 wt%Ni/3 wt%MgO-Al_2O_3 catalysts. Reaction conditions: $CH_4/CO_2 = 1$, GHSV = 12000 mL/(g_{cat}·h), time on the stream = 300 min

4. Conclusions

Ni/MgO-Al_2O_3 catalysts with different Ni loadings (5 wt%, 10 wt%, 15 wt% and 20 wt%) were prepared and employed in CO_2 reforming of methane. The results showed that the catalytic activity increased with the increase of Ni loading because of providing more accessible Ni active sites. In addition, by increasing Ni loadings, the catalyst could be reduced in lower temperatures due to the increase of Ni particle size and decrease of the interaction between Ni and the support. Also by increasing Ni contents, coke formation increased in MgO modified Ni/Al_2O_3 catalysts.

Acknowledgements

The authors are grateful to University of Kashan for supporting this work by Grant No. 158426/16.

References

[1] Chen W, Zhao G F, Xue Q S, Chen L, Lu Y. *Appl Catal B*, 2013, 136-137: 260
[2] Alipour Z, Rezaei M, Meshkani F. *J Ind Eng Chem*, 2014, 20(5): 2858
[3] Zanganeh R, Rezaei M, Zamaniyan A. *Int J Hydrog Energy*, 2013, 38(7): 3012
[4] Sun Y, Collins M, French D, McEvoy S, Hart G, Stein W. *Fuel*, 2013, 105: 551
[5] Hadian N, Rezaei M, Mosayebi Z, Meshkani F. *J Nat Gas Chem*, 2012, 21(2): 200
[6] Arandiyan H, Li J H, Ma L, Hashemnejad S M, Mirzaei M Z, Chen J H, Chang H Z, Liu C X, Wang C Z, Chen L. *J Ind Eng Chem*, 2012, 18(6): 2103
[7] Meshkani F, Rezaei M. *J Nat Gas Chem*, 2011, 20(2): 198
[8] Hou Z, Yokota O, Tanaka T, Yashima T. *Appl Catal A*, 2003, 253(2): 381
[9] García-Diéguez M, Herrera M C, Pieta I S, Larrubia M A, Alemany L J. *Catal Commun*, 2010, 11(14): 1133
[10] Ranjbar A, Rezaei M. *Int J Hydrog Energy*, 2012, 37(8): 6356
[11] Zhu J Q, Peng X X, Yao L, Tong D M, Hu C W. *Catal Sci Technol*, 2012, 2(3): 529
[12] Xu L L, Song H L, Chou L J. *Appl Catal B*, 2011, 108(1-2): 177
[13] Shekhawat D, Spivey J J, Berry D A. Fuel Cells: Technologies for Fuel Processing. UK: Elsevier, 2011. 191
[14] Al-Fatesh A S A, Fakeeha A H, Abasaeed A E. *Chin J Catal (Cuihua Xuebao)*, 2011, 32(10): 1604
[15] Sutthiumporn K, Kawi S. *Int J Hydrog Energy*, 2011, 36(22): 14435
[16] Zhu J Q, Peng X X, Yao L, Shen J, Tong D M, Hu C W. *Int J Hydrog Energy*, 2011, 36(12): 7094
[17] Wang S B, Lu G Q M. *J Chem Technol Biotechnol*, 2000, 75(7): 589